PHYSICAL REVIEW B VOLUME 44, NUMBER 20 15 NOVEMBER 1991-II

Dynamics of subsurface and surface chemisorption for B, C, and N on GaAs and InP

Madhu Menon
Department of Physics, University of Kentucky, Lexington, Kentucky 40506

Roland E. Allen
Center for Theoretical Physics, Department of Physics, Texas A&M University, College Station, Texas 77843
(Received 28 December 1990)

Using Hellmann-Feynman molecular-dynamics simulations, we have investigated interactions of first-row elements with the (110) surfaces of GaAs and InP. We find that these atoms prefer to occupy subsurface sites. The open structure of the tetrahedrally bonded GaAs and InP, together with the small sizes of the first-row elements, makes it relatively easy for these atoms to move beneath the surface. Surface chemisorption is also observed in the simulations, but is found to be metastable.

I. INTRODUCTION

Several years ago, we predicted that small atoms like B will chemisorb at subsurface sites on III-V semiconductors.[1,2] Subsequently, it has been found in scanning tunneling microscopy (STM) and synchrotron x-ray-diffraction studies that B occupies a subsurface site on Si(111).[3–7] We regard this as a confirmation of the prediction, since the diamond structure of Si is essentially the same as the zinc-blende structure of the III-V semiconductors, and the chemistry is also similar.

In this paper we report further studies of first-row atoms on III-V semiconductors—B, C, and N on the (110) surfaces of GaAs and InP. We again observe subsurface chemisorption, on a short time scale (~ 1 ps). Also, total-energy calculations indicate that the subsurface sites are more stable than the sites associated with surface chemisorption. These findings can be rationalized through geometrical arguments. The zinc-blende structure (and the diamond and wurtzite structures) are very open, because of the fourfold covalent bonding. It is therefore relatively easy for a small, first-row atom to slip beneath the surface. Also, the chemisorbing atom is "happier" in the subsurface site, because it has a higher coordination. Our results, however, are based on detailed computer simulations using Hellmann-Feynman molecular dynamics. One of our findings is that the dynamics of subsurface chemisorption involves a concerted motion of semiconductor atoms and adsorbing atom, i.e., the semiconductor atoms move out of the way as the foreign atom moves into the surface. The forces are also many-body, determined from the global energy of the system through the Hellmann-Feynman theorem.

After an adsorbed atom has found a subsurface site, the surface atoms have been displaced from their initial positions. The main result is an outward displacement of the semiconductor atom immediately above the foreign atom (~ 0.5 Å or more), but some semiconductor atoms undergo an inward displacement. Our prediction of subsurface chemisorption should therefore be testable with STM, since there should be a strong perturbation of the original surface relaxation, rather than an extra atom atop the surface.

II. TECHNIQUE

Our technique involves computation of the atomic forces directly from the electronic structure of the entire system. Details of this technique have been presented elsewhere.[8–11] Here we briefly outline the method, and also introduce a feature that reduces the computer time by a factor of 2.

If the total energy U of a system is known, the force F_x associated with an atomic coordinate x is given by

$$F_x = -\frac{\partial U}{\partial x} . \tag{2.1}$$

One can then easily do molecular-dynamics simulations by numerically solving Newton's equation

$$m\frac{d^2x}{dt^2} = F_x \tag{2.2}$$

to obtain x as a function of time.

There are four contributions to the total energy U:

$$U = U_{\rm el} - U_{\rm ee} + U_{\rm ions} + U_{\rm xc} . \tag{2.3}$$

$U_{\rm el}$ is the sum of the one-electron energies ε_k,

$$U_{\rm el} = \sum_k^{\rm occ} \varepsilon_k \tag{2.4}$$

which double counts the Coulomb interaction $U_{\rm ee}$, but omits the ion-ion repulsion $U_{\rm ions}$ and the exchange-correlation energy $U_{\rm xc}$. We approximate these remaining terms in (2.3) by a repulsive pair potential $\phi(r)$:

$$U_{\rm rep} = U_{\rm ions} - U_{\rm ee} + U_{\rm xc} \tag{2.5}$$

with

$$U_{\rm rep} = \sum_i \sum_{j\,(>i)} \phi(r_{ij}) . \tag{2.6}$$

Here, r_{ij} is the separation of atoms i and j. The electronic energies ε_k are approximated by a semiempirical tight-binding Hamiltonian, whose parameters are taken to scale exponentially with the distance r.[10] The repulsive potential is assumed to decrease exponentially with

 ©1991 The American Physical Society

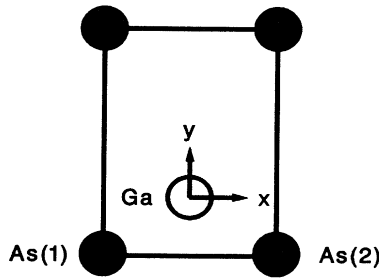

FIG. 1. Top view of the GaAs(110) surface, with choice of coordinates and labeling of atoms.

r-d, where d is the sum of the covalent radii of the interacting atoms, and cutoffs are imposed in both cases. We use Harrison's universal tight-binding parameters and effective atomic energies[12] in (2.4). Although the values of total energies are somewhat sensitive to the choice of parameters, the forces and ordering of relative minima are found to be less affected.

Treating the interactions of atoms with a finite region of a semi-infinite crystal requires some care. Techniques based on two-dimensional periodicity are inappropriate, and cluster models are inaccurate. We have developed a technique that employs Green's-function methods. In this technique, a cluster Hamiltonian H_{cl} is replaced by a "subspace Hamiltonian" $H_{sub}(\varepsilon)$, for a subspace of a finite number of atoms at the surface of a semi-infinite crystal.

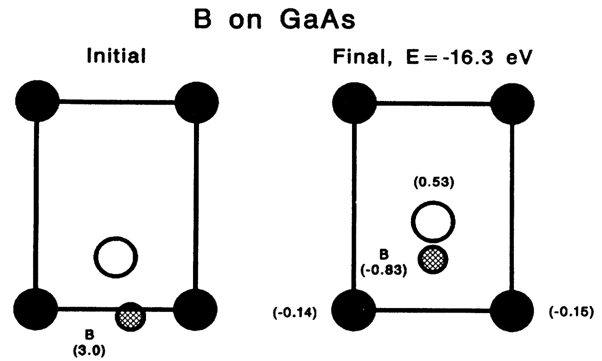

FIG. 2. Initial and final stages of simulation for boron on GaAs.

Let $\underline{H}$ be the $N \times N$ Hamiltonian matrix for a large system ($N \rightarrow \infty$ here). We suppose that $\underline{H}$ differs from an unperturbed Hamiltonian $\underline{H}_0$ only in some $n \times n$ block, where $n \ll N$:

$$\underline{H} = \underline{H}_0 + \underline{V} , \tag{2.7}$$

$$\underline{V} = \begin{bmatrix} V^{11} & 0 \\ 0 & 0 \end{bmatrix} . \tag{2.8}$$

The Green's function for this system is

$$\underline{G} = (\varepsilon \underline{1} - \underline{H})^{-1} . \tag{2.9}$$

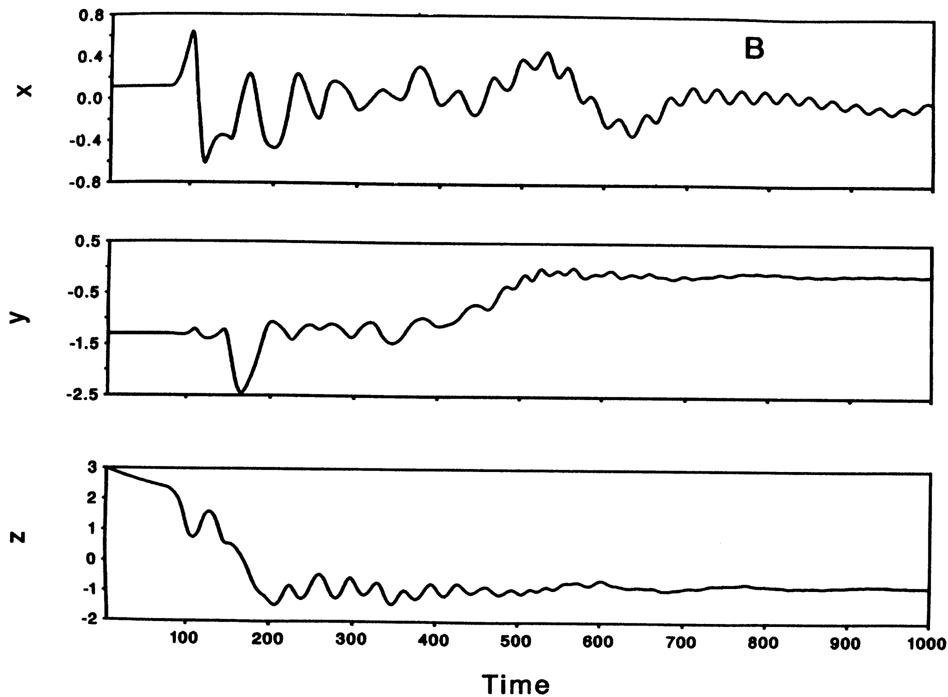

FIG. 3. Detailed motion graph of B moving into GaAs. (The time unit is 1.04×10^{-15} sec for GaAs; the unit of length is half the bond length, which is 1.225 Å for GaAs.)

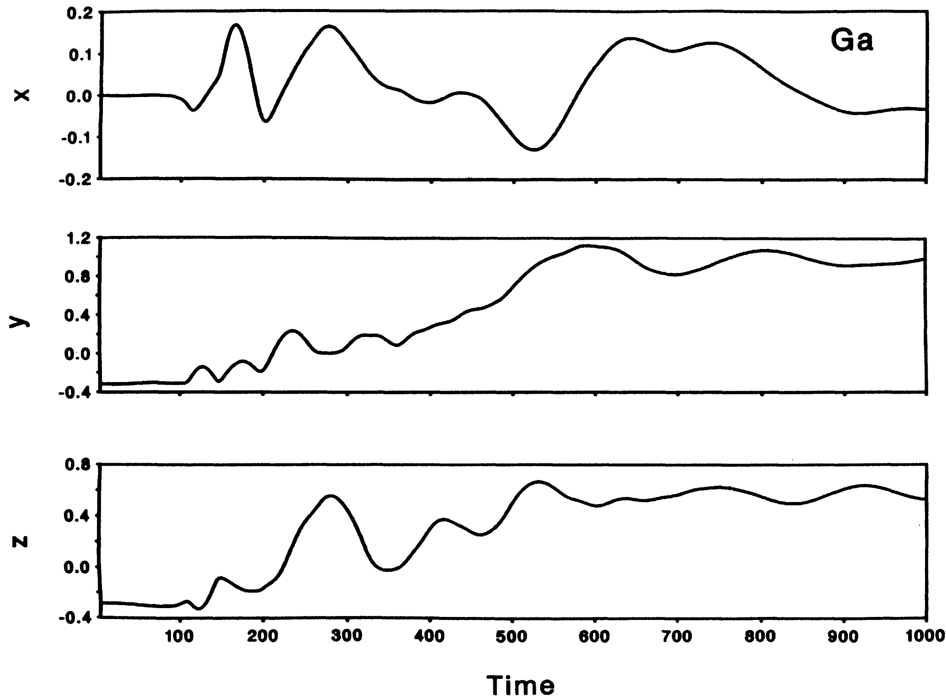

FIG. 4. Response of surface Ga atom to B. (Same units as in Fig. 3.)

We then partition $\underline{H}$ and $\underline{G}$ in the same way as $\underline{V}$,

$$\underline{H}=\begin{bmatrix} H^{11} & H^{12} \\ H^{21} & H^{22} \end{bmatrix} , \tag{2.10}$$

$$\underline{G}=\begin{bmatrix} G^{11} & G^{12} \\ G^{21} & G^{22} \end{bmatrix} , \tag{2.11}$$

and for simplicity in notation define $V=V^{11}$, $H=H^{11}$, and $G=G^{11}$.

Let $\underline{G}_0$ be the unperturbed Green's function corresponding to $\underline{H}_0$ and let $G_0=G_0^{11}$. We then define the subspace Hamiltonian by

$$\varepsilon-H_{\rm sub}(\varepsilon)=G_0^{-1}-V \ . \tag{2.12}$$

In general, $H_{\rm sub}$ is non-Hermitian and energy dependent, with right and left eigenvectors ψ_i and $\overline{\psi}_i$:

$$H_{\rm sub}(\varepsilon)\psi_i(\varepsilon)=\varepsilon_i(\varepsilon)\psi_i(\varepsilon) \ , \tag{2.13a}$$

$$H_{\rm sub}^{\dagger}(\varepsilon)\overline{\psi}_i(\varepsilon)=\varepsilon_i^{*}(\varepsilon)\overline{\psi}_i(\varepsilon) \ . \tag{2.13b}$$

The derivatives of the eigenvalues of ε_i with respect to an atomic coordinate x are given by the Hellmann-Feynman theorem[8,9]

$$\frac{\partial\varepsilon_i(\varepsilon)}{\partial x}=\overline{\psi}_i^{\dagger}(\varepsilon)\frac{\partial V}{\partial x}\psi_i(\varepsilon) \ . \tag{2.14}$$

With the use of (2.9)–(2.12), and two matrix inversions, $H_{\rm sub}$ can be represented in terms of the partitioned matrix of (2.10) as

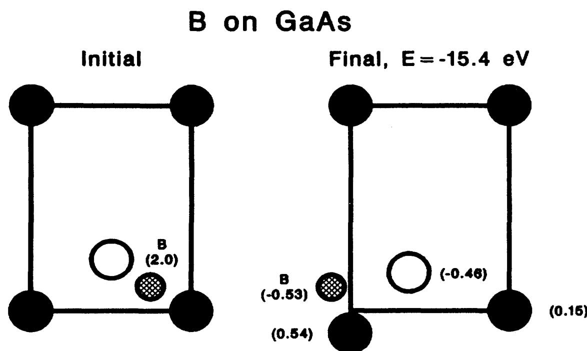

FIG. 5. Another simulation for B, exhibiting subsurface chemisorption on GaAs, with different initial conditions.

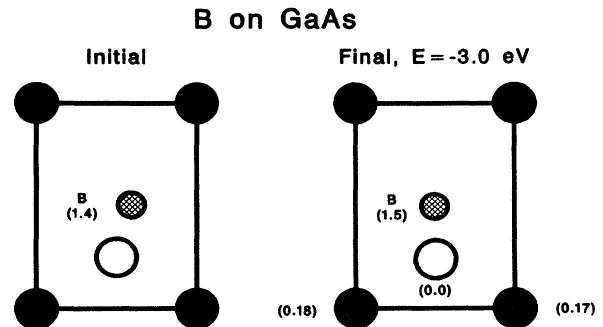

FIG. 6. B chemisorption above the GaAs surface.

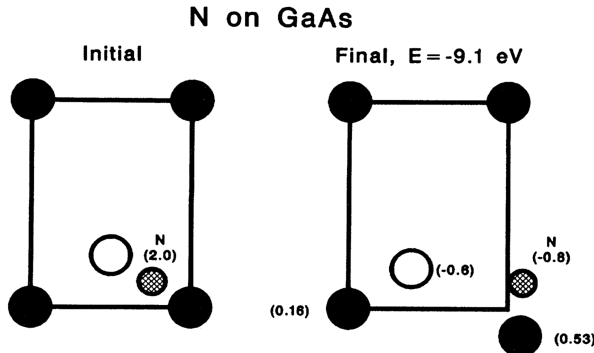

FIG. 7. Subsurface chemisorption of N on GaAs.

$$H_{\rm sub}(\varepsilon)=H+H^{12}(\varepsilon-H^{22})^{-1}H^{21} \ . \quad (2.15)$$

In this form $H_{\rm sub}$ is identical to the effective Hamiltonian of Löwdin and Pryce.[9] Since all the matrices of (2.10) are real and symmetric, $H_{\rm sub}$ is symmetric, and non-Hermitian only when ε is complex. (When a real ε lies in a band of energies, it must be replaced by $\varepsilon+i\delta$, $\delta\to 0$, so $H_{\rm sub}$ becomes non-Hermitian within a continuum of bulk or surface states.) In general, however, we have $H^T_{\rm sub}=H_{\rm sub}$, or

$$H^\dagger_{\rm sub}(\varepsilon)=H^*_{\rm sub}(\varepsilon) \ . \quad (2.16)$$

Taking the complex conjugate of (2.13a) then gives

$$H^\dagger_{\rm sub}(\varepsilon)\psi_i^*(\varepsilon)=\varepsilon_i^*(\varepsilon)\psi_i^*(\varepsilon) \ . \quad (2.17)$$

Comparing this with (2.13b), we see that

$$\bar{\psi}_i(\varepsilon)=\psi_i^*(\varepsilon) \quad (2.18a)$$

and

$$\bar{\psi}_i^\dagger(\varepsilon)=\psi_i^T(\varepsilon) \ . \quad (2.18b)$$

Equation (2.14) can now be simplified:

$$\frac{\partial\varepsilon_i(\varepsilon)}{\partial x}=\psi_i^T(\varepsilon)\frac{\partial V}{\partial x}\psi_i(\varepsilon) \ . \quad (2.19)$$

This translates into a factor-of-2 reduction in computer time, since one does not have to solve the eigenvalue problem separately for $H^\dagger_{\rm sub}$. The expression for the force associated with a coordinate x can be written[9]

$$F_x=\frac{1}{\pi}{\rm Im}\sum_i\int_C\frac{d\varepsilon}{\varepsilon-\varepsilon_i(\varepsilon)}\frac{\partial\varepsilon_i(\varepsilon)}{\partial x} \ . \quad (2.20)$$

Since we are using an sp^3 tight-binding model, there are four orbitals associated with each atom. Our perturbed electronic subspace has nine atoms. Thus the relevant matrices are each 36×36. The electronic effects of all the remaining atoms in the semi-infinite crystal are included via the second term in (2.15).

III. RESULTS

We now present results for first-row elements deposited on GaAs and InP. Figure 1 shows a top view of the (110) surface for the case of GaAs. The z axis points out of the

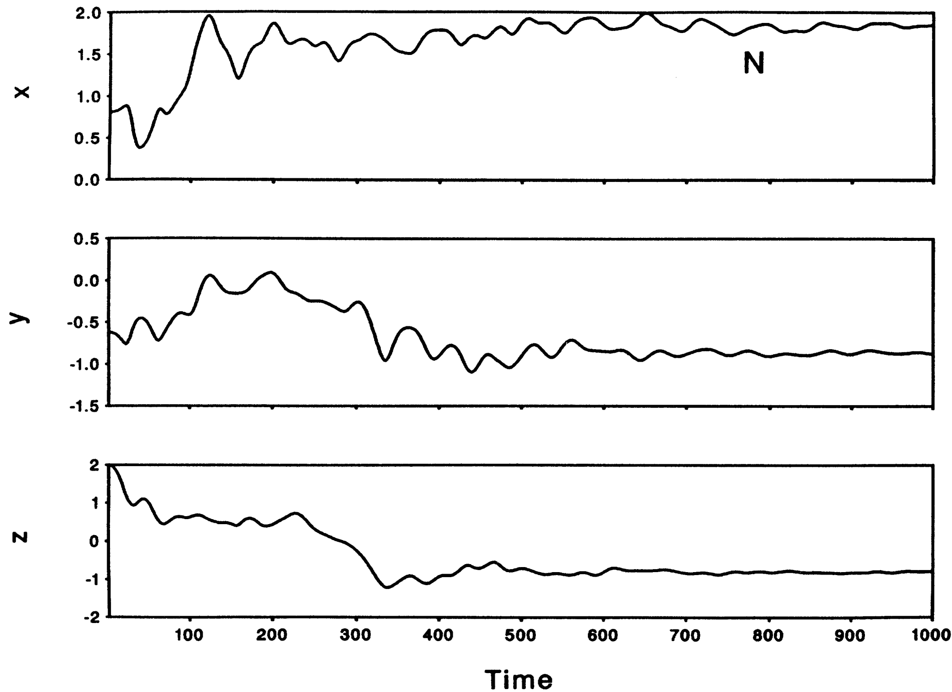

FIG. 8. Detailed motion graph for the inward motion of N in Fig. 7. (Same units as in Fig. 3.)

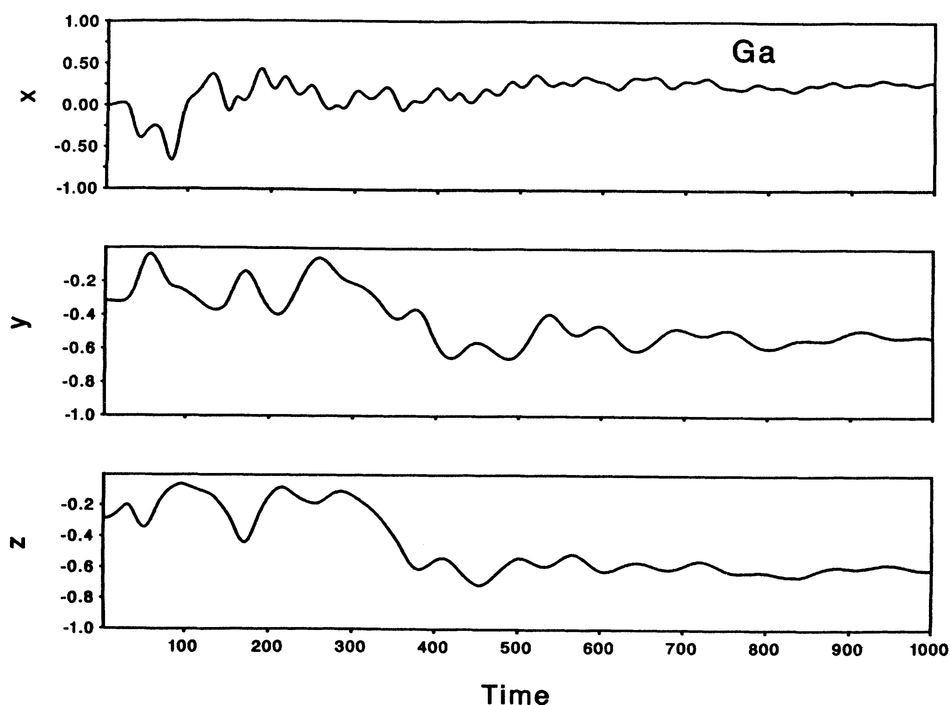

FIG. 9. Response of the surface Ga atom to the inward motion of N in Fig. 7. (Same units as in Fig. 3.)

surface, and the unit of length is taken to be half the bond length—1.225 Å for GaAs and 1.27 Å for InP. The unrelaxed position of the Ga atom is taken to be the origin. The As atoms at the lower and upper right corners then have coordinates (1.63,–1.15,0) and (1.63,3.45,0), respectively, before they are allowed to relax. The unit of time is 1.04×10^{-15} sec for GaAs and 0.91×10^{-15} sec for InP.

In all of the present simulations, the surface atoms are initially at their relaxed positions. (We use our calculated

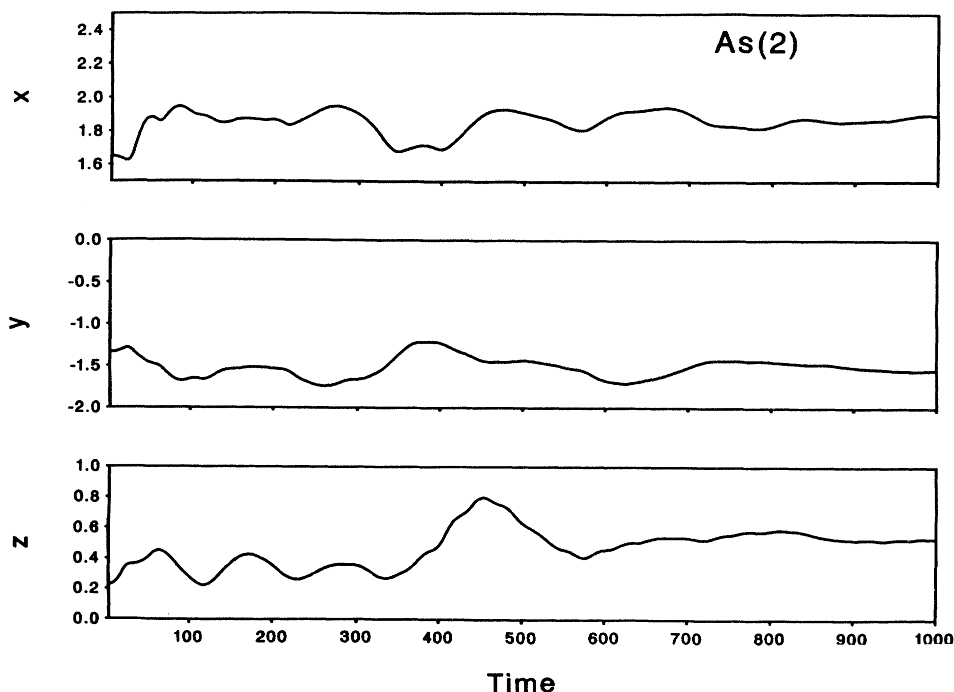

FIG. 10. Response of the surface As atom in the simulation of Fig. 7. (Same units as in Fig. 3.)

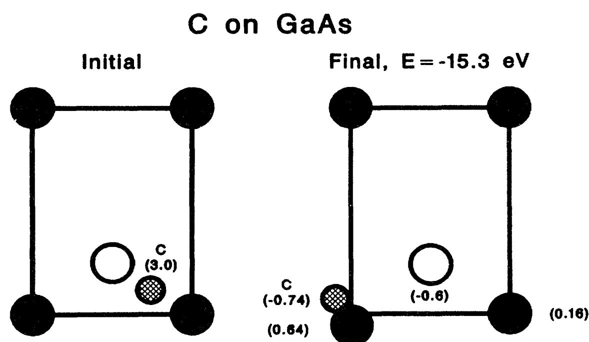

FIG. 11. Subsurface chemisorption of C on GaAs.

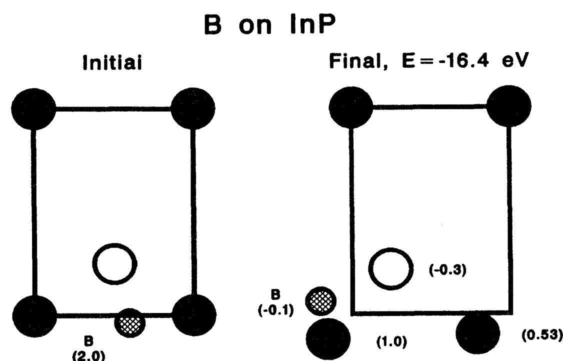

FIG. 12. Initial and final stages of simulation for B on InP.

relaxations, which are close to the experimentally observed relaxations.) Each velocity is reduced by 0.5% at each time step, in order to reach an equilibrium configuration in a reasonable amount of time. The time step is taken to be the same as the unit of time. All the simulations presented in this paper are for 1000 time steps, or approximately 1 ps.

In Fig. 2, we show the initial and final configurations for a simulation of boron on GaAs. The numbers in parentheses represent the z coordinate, with the unit of length defined above. The incident boron atom is given a small velocity toward the surface. At the end of this simulation, the B occupies a position under the surface Ga atom, which is pushed upward from its relaxed position. It is also displaced in the y direction. The two nearest As atoms relax inward, however. (Recall that when the surface is relaxed, the As atoms occupy positions slightly above the surface, with the Ga atoms slightly below.) As will be seen in the following, this general qualitative outcome is also observed in the other simulations that result in subsurface chemisorption: the surface atom directly above the foreign atom protrudes outward, while other surface atoms bonded to the foreign atom are pulled inward, forming a roughly pyramidlike structure.

The detailed motion of the B, leading to the final configuration of Fig. 2, is shown in Fig. 3, and provides some useful insights into the dynamics of subsurface chemisorption. Moving toward the surface with a small velocity, it is initially attracted by a surface As atom (lower right atom in Fig. 1). At the closest point of encounter, it is repelled. It then moves toward the Ga atom, pushing it away and moving beneath the surface,

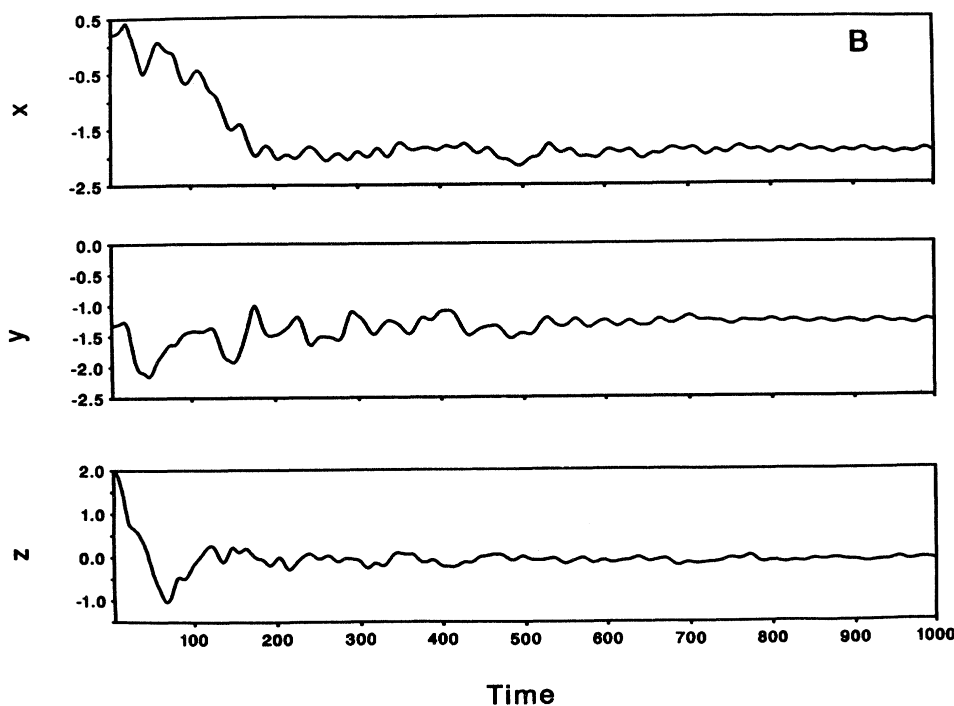

FIG. 13. Detailed motion graph of B moving into InP. (The time unit is 0.91×10^{-15} sec for InP; the unit of length is half the bond length, which is 1.27 Å for InP.)

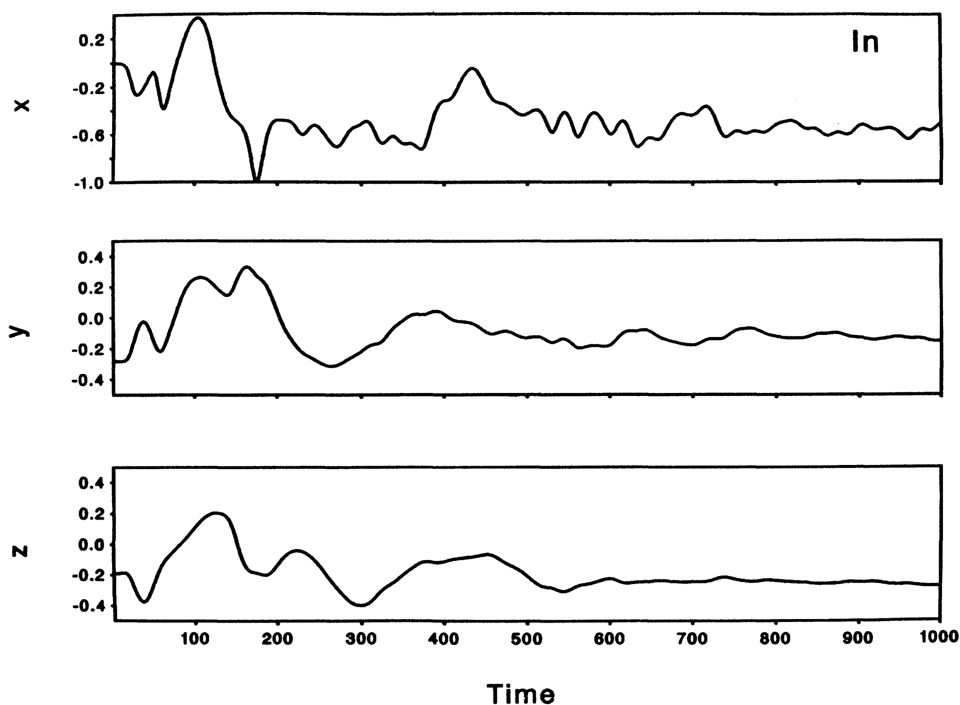

FIG. 14. Response of surface In atom to B motion. (Same units as in Fig. 13.)

where it finds a stable equilibrium position.

The response of the Ga atom is shown in Fig. 4. Initially relaxed inward, it is displaced upward and over to make room for the boron. Finally, after large excursions, it settles into a new equilibrium position. Subsurface chemisorption is thus a classical many-body phenomenon, involving correlated motion of all the interacting atoms.

Figure 5 shows a simulation for boron with different initial conditions. Here the boron atom is released at a

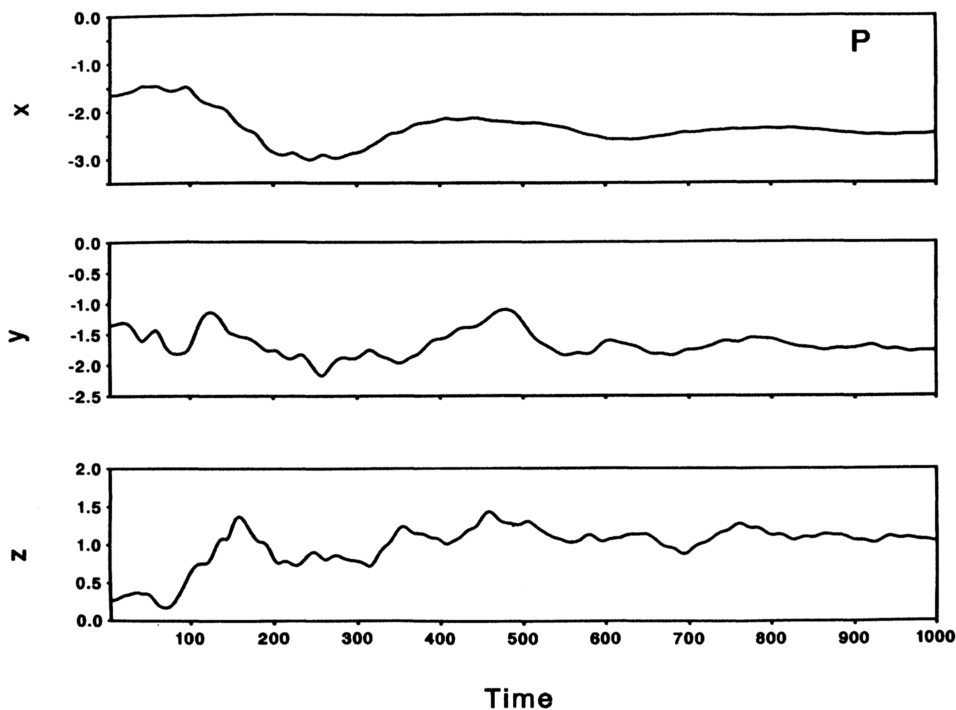

FIG. 15. Response of the surface P atom under which the B of Fig. 12 bonds. (Same units as in Fig. 13.)

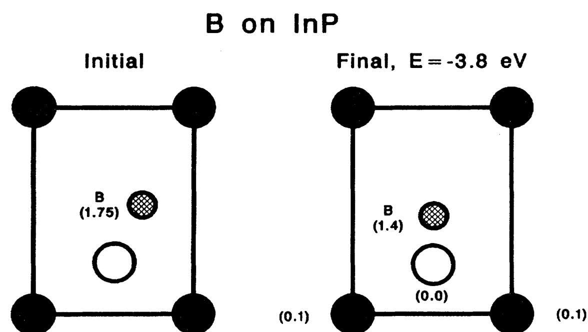

FIG. 16. B chemisorption above the InP surface.

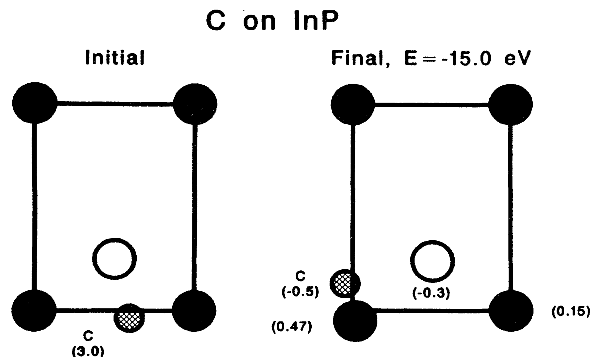

FIG. 17. Subsurface chemisoprtion of C on InP.

different position on the surface, with no initial velocity. It finds an equilibrium position under a surface As atom, which is pushed up. The nearby Ga atom is pulled down, along with a Ga atom on the left (not shown). In Fig. 6, with different initial conditions, the boron chemisorbs above the surface. However, the energy is much higher than in Figs. 2 and 5, i.e., the subsurface sites are energetically highly preferred.

In Fig. 7, we show a simulation for N released with zero initial velocity. It breaks the bond between the surface Ga and As atoms as it moves into the substrate.

Figures 8, 9, and 10 show, respectively, the detailed motion graphs for this nitrogen, the response of the Ga atom, and the response of one As atom [As(2)].

In Fig. 11, we show a simulation for a carbon atom released directly above a Ga-As bridge site, with a small initial velocity toward the surface. This carbon atom moves in and settles under a surface As atom, at the end of 1 ps. The As atom is pushed up from its initial relaxed position, while the nearby Ga is pulled downward, exhibiting the same qualitative behavior as in the previous simulation.

We now turn to InP. The size mismatch caused by the larger covalent radius of In and the smaller covalent radius of P, along with the mass mismatch, gives rise to some interesting effects, both in the dynamics and in the final configurations.

Figure 12 shows a simulation for boron on InP. The boron is released one bulk InP bond length (2.54 Å) above the surface, without any initial velocity. At the end of the simulation, lasting for about 1 ps, it has moved under one of the P atoms, pushing it half a bond length outward. Note that P here occupies a position higher above the surface than its counterpart As in GaAs, whereas the In is pulled into the substrate only slightly compared to its counterpart Ga in GaAs. This difference presumably results from the much larger ratio of cation to anion size.

The detailed motion graphs for B, In, and P, leading up to the final configuration in Fig. 12, are shown, respectively, in Figs. 13, 14, and 15. B always shows large frequency oscillations because of its small mass. Notice that motion to a subsurface site has occurred much more quickly than for GaAs with identical initial conditions. We have found that inward motion occurs relatively easily on InP in numerous other simulations, with different initial conditions and various first-row atoms. The detailed motion graph for In, in Fig. 14, shows a large excursion near the 100th time step, as the boron moves down. P moves upward to accommodate the boron underneath.

Figure 16 shows another simulation for B, with different initial conditions. Here the boron bonds above the surface to a single In atom. The energy for this configuration is much larger, i.e., again subsurface chemisorption is energetically more favorable than chemisorption on the surface.

A simulation for C on InP is shown in Fig. 17. Once again, subsurface chemisorption is observed, but the final positions are considerably different than for either B on InP or C on GaAs.

IV. CONCLUSIONS

The detailed simulations reported here lead to several conclusions, some of which are experimentally testable.

(1) For the small atoms B, C, and N adsorbing on surfaces of tetrahedrally bonded semiconductors—GaAs(110) and InP(110) in the present simulations—subsurface chemisorption is achieved quickly.

(2) In these systems, subsurface chemisorption is energetically more stable than chemisorption above the surface.

(3) Typically, the surface atom immediately above the foreign atom protrudes upward by ~ 0.5 Å, while the other surface atoms bonded to the foreign atom undergo inward displacements.

(4) The dynamics of the chemisorption event involves a concerted motion of foreign atom and semiconductor atoms.

(5) Subsurface chemisorption proceeds more easily on InP than on GaAs, because of the size mismatch.

Although only GaAs and InP have been considered here, they are representative of tetrahedrally bonded semiconductors, and the results reported in this paper are in qualitative agreement with recent investigations of boron at the Si(111) surface.[3-7]

ACKNOWLEDGMENTS

This work was supported by the U.S. Office of Naval Research, Grant No. N00014-91-J-1126, and the Robert A. Welch Foundation (Houston, Texas). Computer time was provided by a grant from Cray Research, Inc.

[1]M. Menon and R. E. Allen, Surf. Sci. **197**, L237 (1988).
[2]M. Menon and R. E. Allen, in *The Structure of Surfaces II,* edited by J. F. van der Veen and M. A. van Hove (Springer-Verlag, Berlin, 1988).
[3]R. L. Headrick, I. K. Robinson, E. Vlieg, and L. C. Feldman, Phys. Rev. Lett. **63**, 1253 (1989).
[4]P. Bedrossian, R. D. Meade, L. Mortensen, D. M. Chen, J. A. Golovchenko, and D. Vanderbilt, Phys. Rev. Lett. **63**, 1257 (1989).
[5]I.-W. Lyo, E. Kaxiras, and Ph. Avouris, Phys. Rev. Lett. **63**, 1261 (1989).
[6]H. Huang, S. Y. Tong, J. Quinn, and F. Jona, Phys. Rev. B **41**, 3276 (1990).
[7]E. Kaxiras, K. C. Pandey, F. J. Himpsel, and R. M. Tromp, Phys. Rev. B **41**, 1262 (1990).
[8]M. Menon and R. E. Allen, Bull. Am. Phys. Soc. **30**, 362 (1985).
[9]R. E. Allen and M. Menon, Phys. Rev. B **33**, 7099 (1986).
[10]M. Menon and R. E. Allen, Phys. Rev. B **38**, 6196 (1988).
[11]M. Menon and R. E. Allen, J. Vac. Sci. Technol. B **7**, 729 (1989), and references therein.
[12]W. A. Harrison, *Electronic Structure and the Properties of Solids* (Freeman, San Francisco, 1980), and references therein.